

Chapter

Advanced HF Communications for Remote Sensors in Antarctica

Joaquim Porté, Joan Lluís Pijoan, Josep Masó, David Badia, Agustín Zaballos and Rosa Maria Alsina-Pagès

Abstract

The Antarctica is a continent mainly devoted to science with a big amount of sensors located in remote places for biological and geophysical purposes. The data from these sensors need to be sent either to the Antarctic stations or directly to the home country. For the last 15 years, La Salle has been working in the application of HF communications (3–30 MHz) with ionospheric reflection for data collection of remote sensors in Antarctica. We have developed and tested the several types of modulations, the frame structure, the radio-modem, and the antennas for two different scenarios. First, a long-range transequatorial (approximately 12,800 km) and low-power communication system is used as an alternative to satellites, which are often not visible from the poles. This distance is covered with a minimum of four hops with oblique incidence in the ionosphere. Second, a low-power system using near vertical incidence skywave (NVIS) communications provides coverage in a surface of approximately 200–250 km radius, a coverage much longer than any other systems operating in either the VHF or UHF band without the need of line of sight.

Keywords: atmosphere science, ionospheric propagation, HF, NVIS, remote sensing, advanced modulations

1. Introduction

There is a strong research activity in Antarctica in the fields of geophysics, meteorology, wildlife, flora, oceanography, and environment, among others. This research activity often involves the installation of sensors in remote places under severe/extreme weather conditions. Most of those sensors are operated with a data logger that stores the data between campaigns until it is recovered after several months.

If we need either to have access to the data throughout the year, or to install a sensor far away from the Antarctic station, we should install a radio transmission system. The standard VHF radios have a reach up to 50 km with line of sight. As the installation of a repeater station is not an option in Antarctica, it only remains to install either a satellite link or an HF link. The satellite services are expensive and are provided mostly by geostationary satellites. The geostationary orbits around the equator are not always easily visible from the poles, so the link is not fully reliable.

The HF band (3–30 MHz) is well known from the beginning of the age of the radio. The ionization of the upper layers of the atmosphere changes the direction of the radio waves in that band, so the ionosphere behaves as a mirror for a certain set

of frequencies. The reflection is strongly dependent on the solar activity, the solar radiation at any time, the terrestrial magnetic field, and the angle of incidence of the wave [1]. For oblique incidence, a range up to 3000 km for a single hop can be achieved, so we can establish a link all over the planet with a few hops. The antenna in those applications should have a maximum of radiation toward the horizon.

For near vertical incidence skywave (NVIS), we can achieve a circular coverage area with a radius up to 250 km without the need of line of sight. The most suitable frequency for vertical incidence is lower than in oblique incidence, so a larger size of the antenna is needed. The antenna should have a maximum of radiation upward, so horizontal dipoles, inverted V, and loops are the best options [2]. As the distance is much lower, the transmission power required can be reduced to tens of Watt, so the application to remote sensors with power restrictions is straightforward. In the world where an increasing number of devices are going to be interconnected in an Internet of Things paradigm, a system able to communicate sensors located hundreds of kilometers away without any additional infrastructure is really welcomed.

A first step when developing a new physical layer is the sounding and characterization of the channel. Apart from the classical model of Watterson [3] for narrowband communications and Mastrangelo [4] for wideband communications, a significant amount of research has been done in ionospheric channels for a single hop at high latitudes in the Arctic [5–7]. However, few works can be found about channel sounding for long-range links with multiple hops from the Antarctica.

For the last 15 years, our research group has been working in the application of HF communications (3–30 MHz) with ionospheric reflection for data collection of remote sensors in Antarctica. In particular, we have developed a system to communicate the Spanish Antarctic Station (SAS) Juan Carlos I at Livingston Island (62.6°S, 60.4°W) and the Ebre Observatory in Roquetes (Tarragona, Spain) (40.8°N, 0.5°E). It is a 12,700 km link with multiple hops and without the use of any repeater. First, we started to sound the channel and estimate the main parameters of the channel [8–12]. Then, we have developed and tested a wide range of modulations, with its frame structure, the radio-modem, and several antennas for both the long range with oblique incidence and the near vertical incidence scenario [13–17]. We are also developing a self-organized network of NVIS nodes that can handle the delays and the unavailability of the ionospheric channel. The NVIS nodes may behave as a hub able to collect data from other neighboring sensors and transmit the joint data to the central node.

This chapter is organized as follows. In Section 2, the evolution of the hardware of the radio-modem and the antennas is presented. The modem is prepared for both channel sounding and data transmission and has evolved to low-cost software radio platforms. In Section 3, the results of more than 15 years of experience in channel sounding are presented, for both the oblique and the vertical sounding. The variability of the channel as a function of time, season, and year is summarized. In Section 4, the physical layer of the communication system of the modem is introduced. The modulation, the frame structure, and the synchronization techniques for both the long-range modem and the NVIS modem are described. The performance in terms of bit rate and bit-error rate is presented. In Section 5, new routing strategies for NVIS networks are explained. The NVIS node has to collect the data from the sensors nearby and establish a delay tolerant network (DTN) with the rest of the nodes. Finally, Section 6 contains the conclusions and some other applications of HF communications.

2. System

From the beginning of the project, we pursued a software-defined radio (SDR) hardware platform which was able to both sound the ionospheric channel and

implement different modulation schemes without changing the hardware. This kind of platform was not available 15 years ago, so we had to develop our own platform with the FPGAs Virtex-IV and Spartan-II and the fastest ADC and DAC of that time. The control of the whole system and the rest of peripherals was performed by an embedded PC [10]. For the long-range link between the SAS and Spain, the system was able to transmit along the whole HF band (3–30 MHz), 24 hours a day, with two synchronized receivers connected to two wideband antennas: a monopole with antenna tuner and a wideband inverted V. The transmission power was 250 W and the system was designed to work, connected with the main power. The author is referred to [11] for further details of that system.

NVIS communication between remote sensors and the SAS is a quite different challenge. The sensor will be often battery-powered so the transmission power should be as low as possible. Although we started developing our own platform for NVIS [18], we can now find different compact SDR platforms that include FPGA, embedded microprocessor, and AD/DA converters in a very cost-effective platform. The implementation of the low-cost transceiver for remote sensors using NVIS is detailed in the following section.

2.1 The NVIS transceiver

The hardware of the system (see **Figure 1**) is composed by three parts: a Red Pitaya (RP), a Raspberry Pi 3 (Rpi3), and different peripherals.

The RP (FPGA board) is a low-cost SDR platform dedicated to the transmission and reception of the radiofrequency signals, converting them from analog to digital with an ADC of 14 bits, decreasing the frequency of the signal carrier, processing the signal, and sending the low-pass IQ components to the Rpi3 via Ethernet. Similarly, the Rpi3 can send the IQ components to the RP for the transmission. The sampling rate is 125 Ms/s at the RF plane, while it is 100 ks/s at the IQ plane.

Internally, the RP contains a Zynq[®] 7010, based on the Xilinx System on Chip (SoC) architecture. These products integrate a feature-rich dual-core or single-core ARM[®] processing system (PS) and a Xilinx programmable logic (PL) in a single

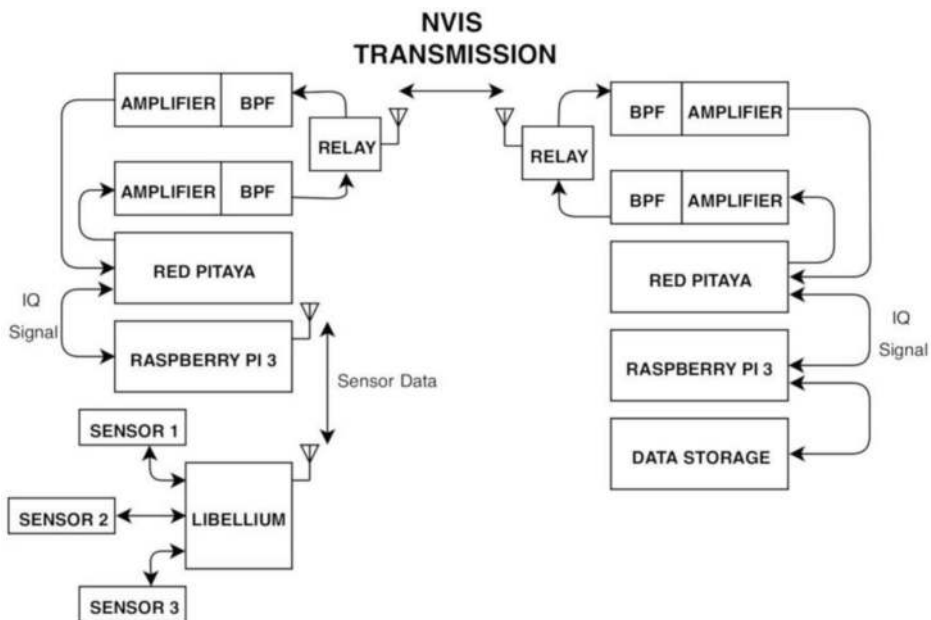


Figure 1.
Block diagram of the NVIS communication system for remote sensors.

device. On the PS, there is a Linux operating system for controlling the PL, where there are all the hardware configurations that allow the different transmission modes.

Although there is a true microprocessor inside the RP, it is not able to handle all the control functions, since the biggest part of the RP is dedicated to the real-time processing in the PL part. That is the reason for adding the Rpi3, a single-board computer that controls the overall system operation. Rpi3 is able to collect data from many wireless sensors connected via Zigbee and encapsulate them on a single frame to be sent through the NVIS channel. In our case, we have used the solution of Libelium [19], with a maximum range between 1 and 8 km, depending on the chosen solution. When Rpi3 either stores 1000 bytes of data or a defined time lapse runs out, it sends the baseband IQ components of the frame to the RP to be transited to the SAS. On the other side, the RP is waiting for reception. When the preamble of the transmission is found, the RP sends the received IQ components to the Rpi3, which demodulates all the data frames and extracts the data from all the sensors.

As mentioned before, the transmission power has to be less than 10 W to ensure a proper operation in a battery-powered scenario. As the maximum output power of the DAC is 0 dBm, we need a linear minimum amplification of 40 dB. The power amplifier is controlled by an electronic circuit that switches the supply voltages of the power stages in the proper order. This hardware measures the forward and reverse power, so the Rpi3 could switch the transmission off in case of mismatch. Finally, a band pass filter (BPF) attenuates the out-of-band emissions.

At the receiver site, another BPF from 2 to 7 MHz is placed close to the antenna to filter all the unwanted noise and interferences typical of the HF band, such as AM broadcast stations. As the received signal may be around -90 dBm, an amplifier of 30 dB is needed in order to take the maximum advantage of the dynamic range of the ADC, without saturating the converter. Finally, the received data are stored in a solid-state disk.

The total measured power consumption of the system is about 7.2 W in sleep mode, which is the dominant mode. Once every hour, the transceiver transmits and receives a few seconds with a power consumption of 96 W. Under these conditions, the transceiver will operate for 2 weeks with a battery of 110 Ah.

2.2 The radiating system

When working in the HF band, we have to expect large-size antennas if we want to achieve dimensions close to half wavelength. If we are going to install the antennas in Antarctica, we will have strict environmental conditions, so no complex installations can be built. Moreover, if the antennas are for remote sensors powered by batteries, we should try to maximize the gain of the antennas in order to reduce the transmission power of the amplifier at minimum. Taking all this into consideration, the best choice are monopoles or wire antennas that need only one elevated point at most.

There is a great difference between the long range with oblique incidence and the near vertical incidence scenario. In the first case, we need a maximum of radiation toward the horizon, so a vertical monopole is the simplest option. In the second case, we need a radiation lobe with elevation angles between 70 and 90° , so the horizontal dipole or the inverted V should work better.

The monopole is the simplest antenna for long-range HF communications. It is easy to carry and install and is very robust against adverse weather conditions. As a wideband antenna, we need an antenna tuner that has to be tuned a low power before every frequency change. As the conductivity of the soil gets worse, the angle of maximum radiation is not 0° any more, but it rises up to 20 – 30° with respect to the horizon [10]. To prevent this, we have to install a set of radials above the soil to

improve its conductivity. In the simulation, for a 7.5 m monopole over a permafrost soil, we demonstrate that 32 radials of 15 m each, we can expect a 2 dB improvement by using radials (see **Figure 2**). In **Figure 3**, we can see the monopole installed in a hill nearby the SAS and a more detailed explanation can be found in [13].

For NVIS applications, the horizontal dipole would be one of the best antennas, but it needs one mast at either end. The inverted V, however, achieves a similar performance with only one mast at the center. For the V of **Figure 4**, we have optimized the height of the antenna (Mast h), the heights of the end (Min h), and the distance from the center to the end (Yf). The length of the V changes accordingly. In **Table 1**, we can see the results for three types of soil: ideal (infinite σ , $\epsilon_r = 6$), rural ($\sigma = 0.01$, $\epsilon_r = 15$), and permafrost ($\sigma = 0.00005$, $\epsilon_r = 3$), where σ and ϵ_r stand for the conductivity and the dielectric constant, respectively, and j is the imaginary unit. The conductivity of the permafrost causes a drop up to 5.5 dB in the gain with respect to the ideal ground. We need a mast height of 13 m to achieve a gain of 1.3 dB. As we want to have a minimum power consumption, we will operate

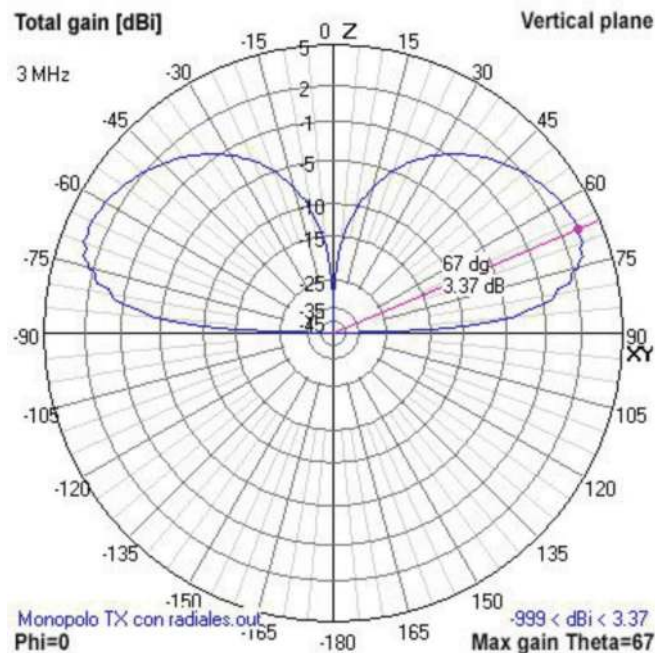


Figure 2.
Diagram of radiation of a 7.5 m monopole with radials over permafrost.



Figure 3.
Installation of the monopole with radials in the SAS.

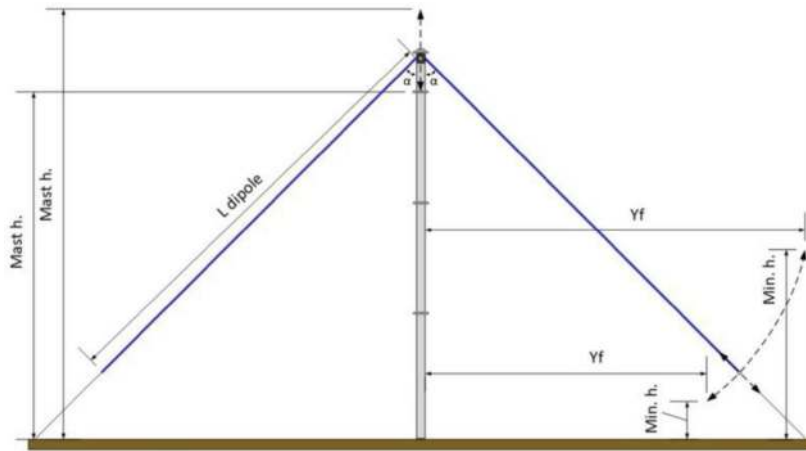


Figure 4.
Simulation parameters of the inverted V.

Soil type	Optimization algorithm	Gain (dBi)	SWR	Impedance (Ω)	Mast h. (m)	Min h. (m)	Yf (m)
Ideal	Evolve	6.8	1.96	$25.6 + 3.2j$	11.01	2.00	12.39
Rural	Evolve	3.8	1.05	$47.7 + 0.4j$	10.81	1.87	12.39
Permafrost	Evolve	1.3	1.27	$63.3 - 1.0j$	13.08	2.00	11.51

Table 1.
Optimization of the inverted V antenna.

at a single frequency and try to maximize the gain at that frequency. So, we do not intend to have a wideband antenna in this scenario. Checking the reports of ionograms of the last decade from Ebre Observatory [20] and Lowell Digisonde International [21], we came to the conclusion that the best frequency for maximum availability would be 4.5 MHz.

It is important to note that the optimization of the gain is a key factor for the transmission, while the radiation diagram with a maximum around 90° and a minimum at the rest of elevation angles is the most important issue in reception, because we minimize the noise and interference from the nondesired directions [22].

As far as the horizontal dipole is concerned, there is a 3 dB gain improvement, bearing in mind that two mast installations are needed. The optimum height, as discussed in [23], is between 0.16λ and 0.22λ depending on the type of soil.

3. Channel sounding

The ionosphere is one of the layers of the upper atmosphere situated between about 90 and 400 km above the surface. Thanks to its atomic composition, the ionic charge allows radiofrequency signals to rebound and go back to the terrestrial surface, thus creating a communication channel. The ionization of this layer is caused by solar radiation producing the apparition of free electrons that change the refraction index of the medium. As more radiation there is, more ions are excited and the maximum reflected frequency increases. As the sun radiation is the major cause of frequency variation, daily, monthly, seasonal, and yearly variations have to be taken into account. Apart from the variation between day and night, one of

the most significant variations is caused by the solar cycle reaching maximum and minimum levels approximately about every 11 years. The sunspot number (SSN) measures the number of spots visible on the face of the sun. The higher the number, the more radiation ionizes this layer of the atmosphere. **Figure 5** shows the variation of the solar cycle radiation from 1995 to 2017, and the estimation until 2019. We can point out that in the current year (2018), solar radiation is in minimum levels. This minimum level causes that the frequency used for the transmissions is much lower than in previous years (between 4.5 and 6.5 MHz during the day).

The ionosphere is observed throughout the world by a set of observatories. Most of them have an ionosonde developed by Lowell Digisonde International [21] and publish the ionogram in a common webpage [25], enabling the parameterization of the ionosphere behavior along the day in quasi-real time.

As the ionosphere is divided into several layers (D, E, F₁, and F₂), which are always moving, the ionospheric channel behaves as a slow fading multipath channel, similar to the wireless channels for mobile communications. Hence, the ionosphere can be characterized by the following parameters: time dispersion (multipath, delay spread), frequency dispersion (Doppler shift, Doppler spread), noise, interferences, and channel availability [26].

All these factors will allow us to determine the best modulations, size of the frame, and occupied bandwidth to optimize the transmission in both the long-range and the NVIS case. In the next two following points, we aim to describe the results of the sounding of both types of communications.

3.1 Oblique sounding results

When we try to characterize a channel, we have to distinguish between the narrowband analysis and the wideband analysis. The narrowband analysis allows us to

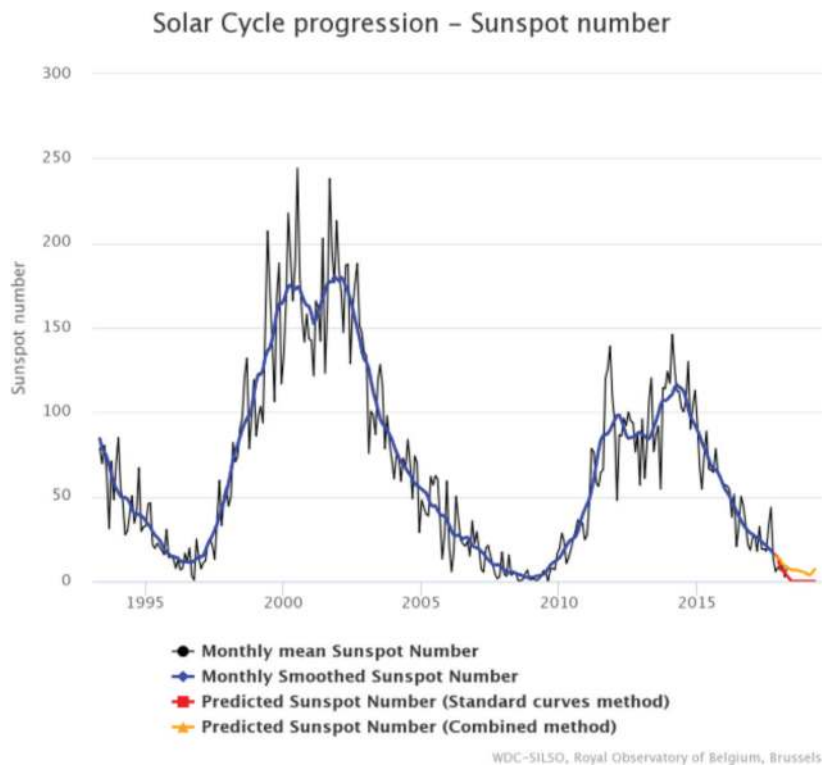


Figure 5.
Evolution of the sunspot number (SSN) [24] from 1995 to 2017.

determine the channel availability and the signal-to-noise ratio (SNR). This sounding is performed with tones that range from 2 to 30 MHz with steps of 500 Hz and are measured with a 10 Hz bandwidth during a time interval of 10 s. We concluded that a good quality of service is achieved for a SNR larger than 6 dB in a 10 Hz of bandwidth [8]. The SNR is measured after filtering the signal with some different windows (Hanning, Blackman, Flattop, Kaiser) defined in [11]. In **Figure 6**, we can see the evolution of the signal envelope during the 10 s transmission interval for each window. The SNR is measured as the ratio between the average of the signal power in case of absence of interference and the noise power measured in the seconds where there is no transmission. The Kaiser window turned out to be the best filtering technique.

The SNR and the channel availability (defined in [8]) are studied as a function of frequency and the time of day (see **Figure 7**). The big differences between day and night and between sunrise and sunset are explained in detail in [11].

The wideband analysis allows the characterization of the rest of the channel parameters such as time and frequency dispersion and wideband SNR. This analysis is performed by sending a pseudorandom noise (PN) sequence that allows us to obtain an estimation of the channel response as a function of time. The channel matrix, that is, the evolution of the channel impulse response over time, is calculated correlating the received signal with the original PN sequence. Then, the scattering function is calculated as the fast Fourier transform (FFT) of the channel matrix. A detailed analysis of the scattering function is key to determine modulation, frame length, separation between data block and data corrector, and other issues of the physical layer [9].

In **Figure 8**, we can see the averaged channel parameters for the campaign 2013–2014. During daytime, high frequencies (20–30 MHz) show the highest delay spread (up to 4 ms) and Doppler spread (up to 1.5 Hz). That means a bigger amount of intersymbolic interference and a higher degree of variability. Sunset and sunrise are the most unstable moments because the ionosphere is changing due to the ion formation or ion recombination. They are, therefore, the least suitable periods for the transmissions. Finally, nighttime is the most stable moment from 19 to 06 UTC.

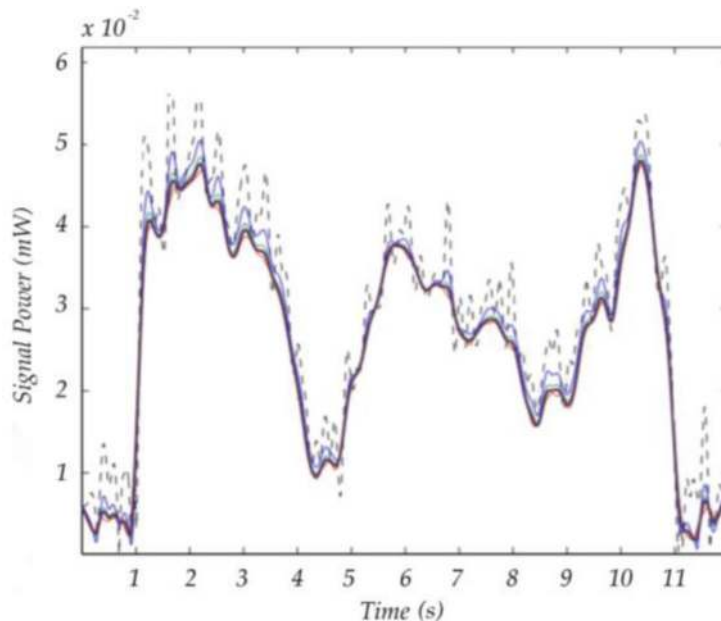


Figure 6.
Time evolution of the signal envelope for narrowband analysis.

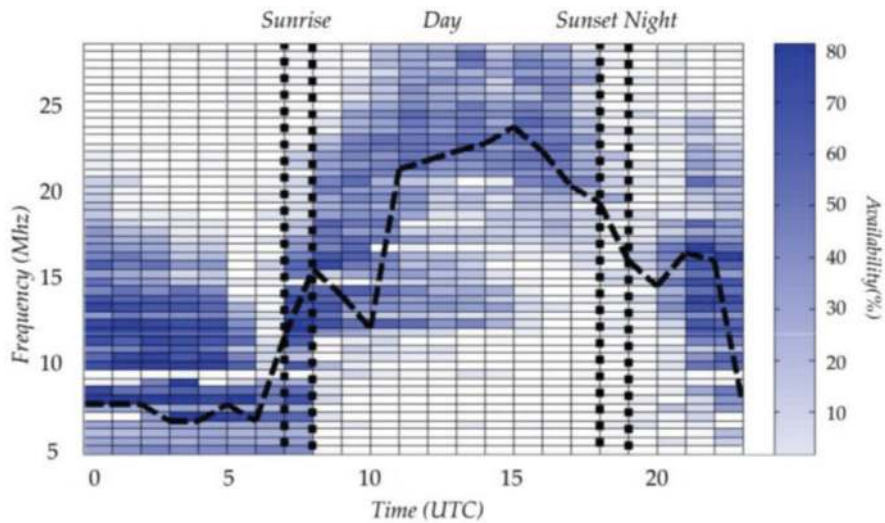


Figure 7. SNR as a function of frequency and time of day (February 17, 2014) during the campaign 2013–2014.

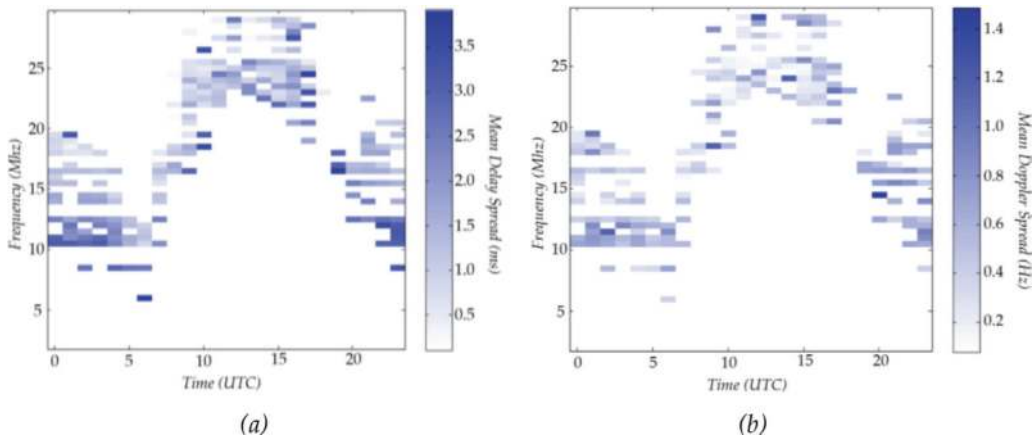


Figure 8. Wideband channel measurements during the campaign 2013–2014: (a) mean of delay spread (in ms); (b) mean of Doppler spread (in Hz).

3.2 NVIS sounding results

For the NVIS channel, there are a few factors to be taken into account. For the narrowband analysis, we only have to check the nearby ionograms and choose the optimum working frequency as the $0.85 \times f_{oF2}$, being f_{oF2} the critical frequency of the upper layer of the ionosphere [27]. For the wideband analysis, we have to notice that the NVIS channel is the same channel that affects the ionosonde when it is measuring the height of the different layers to build the ionogram. The ionosonde temporarily stores a file with the IQ components that is used to calculate the critical frequency, virtual height, and total electron content of each layer. If we have access to this raw data file, we can have an initial estimation of the wideband channel parameters [28]. Of course, an ad hoc channel sounding will yield to better results. In **Table 2**, we can see the studies performed with the raw data of the ionosonde of Ebre Observatory. As expected, both the delay spread and the Doppler spread are lower than in the oblique sounding, so the modulation, the length of the frame, and many other parameters will allow a physical layer with higher transmission capabilities.

Parameters	Wave	October 24, 2012		March 5, 2013	
		Mean	Variance	Mean	Variance
Doppler spread (Hz)	Ordinary	0.681	0.094	0.378	0.199
	Extraordinary	0.123	0.095	0.081	0.061
Doppler shift (Hz)	Ordinary	-0.088	0.554	-0.025	0.208
	Extraordinary	-0.073	0.478	-0.222	0.177
Multipath spread (μ s)	Ordinary	710.71	2.83	496.01	2.02
	Extraordinary	921.41	4.46	712.47	3.19

Table 2.
NVIS sounding results from data of the ionosonde at Ebre Observatory.

4. Physical layer

HF communications are often designed to operate with high-power amplifiers at the transmitter side, with typical values from 1 to 10 kW. When thinking about remote sensors supplied by batteries or solar panels, the transmitted power has to be much lower. For long-range transmissions between the Antarctic stations and Europe, a power value less than 150 W is desirable, while a value less than 30 W is expected for unattended remote sensors installed around the stations.

In a low-power scenario, the modulation has to be extremely robust with respect to noise and interference. Several replicas of the transmitted signal arrive to the receiver due to the reflection at the different layers of the ionosphere. As the layers are in constant motion, the HF channel behaves as a slow-frequency selective channel, so as the mobile channel for wireless communications. Hence, some of the latest techniques applied to the world of mobile telephony can be adapted to HF communications.

For the long-range link (about 12,760 km) with oblique incidence, the SNR at the receiver is extremely poor, often with negative values. In that situation, we defined two different modulation schemes: (i) the robust mode, for SNRs negative or close to zero and (ii) the fast mode, when the SNR is positive, and the bit rate can increase significantly.

In the robust mode, a modulation based on direct-sequence spread spectrum (DS-SS) was designed. The effective net data rate is very low (hundreds of bps), but the data can be demodulated under high levels of noise and interference. In the fast mode, the single carrier-frequency domain equalization (SC-FDE) modulation was used, since it can handle higher data rates (up to 3 kbps) if the different subcarriers can be received at a positive SNR.

For the NVIS link with vertical incidence, the situation is much more suitable. Although the transmitted power is lower, the received signal is higher while the level of interference and noise coming from the vertical direction is reduced significantly. With a SNR between 10 and 20 dB with an available bandwidth of 3 kHz, a narrowband phase shift keying (PSK) or frequency shift keying (FSK) is proposed, achieving bit rates of tens of kbps that ensure another range of applications, such as messaging, e-mail, and digital voice transmission.

When a node is working in an asynchronous mode, the receiver has to be waiting for an incoming signal continuously. A robust signal detector with low false alarm probability has to be developed, with strict requirements of energy consumption. The following subsections deal with the different modulations and the signal detector in detail.

4.1 Modulations for the long-range link

In the oblique transmission from Antarctica, two modulations have been designed for the two reception modes [13]: (i) a DS signaling [15] was designed for high robustness mode and (ii) a SC-FDE for high throughput mode [16].

4.1.1 DS signaling

The spread spectrum tests were performed using a DS-SS signaling modulation. It consists of the use of a whole family of PN sequences [26] and associating each of them to a symbol. The information about the transmission will be contained in the own sequence by means of the use of a codebook. The receiver also has the codebook available and uses it as a dictionary to obtain the transmitted information. The PN sequences used for these tests were gold sequences [29], taking advantage of their low cross-correlation in each family.

The results for the cumulative density function of the bit error rate (BER) results for two thresholds of 5 and 10% are shown in **Table 3**. They present bit rates around hundreds of bits per second—enough for data to be transmitted—and with a reasonable quality assuming that we are facing the most hostile time zone of the channel, the daytime. We found out that the best possible combination is a Gold PN sequence family 2047 length, using a bandwidth of 16.6 kHz and a final bit rate of 89 bps.

4.1.2 SC-FDE

The first tests using SC-FDE were conducted in [16], with the aim of minimizing the problems generated by the peak-to-average power ratio (PAPR) and interchannel interference (ICI) of the previous works using OFDM [17]. The single carrier-frequency domain equalization has been designed with several parameter modifications in comparison with [17], such as variable bandwidth, different length of blocks, and

PN length	T _s (ms)	BW (kHz)	Bit rate (bps)	BER (5%)	BER (10%)
2047	123	16.6	89	0.73	0.81
1023	123	8.3	81	0.66	0.79
511	127	4	73	0.64	0.78
255	127	2	65	0.53	0.67

Table 3.
 Cumulative density function of the BER results for two thresholds of 5 and 10%. Best BER values in bold.

Constellation	T _b (ms)	Bit rate (bps)	Spectral efficiency (bps/Hz)	BER (>0.05)
PSK	10	296.3	0.74	0.54
PSK	30	358.2	0.90	0.56
PSK	50	373.8	0.93	0.57
PSK	70	381.0	0.95	0.39

Table 4.
 Cumulative SC-FDE results for PSK constellation. Best results in bold.

several constellations. The reader is referred to [14] for the results of the extensive tests in SC-FDE, and a synthesis of the best results in terms of the cumulative distribution function (CDF) for a BER greater than 0.05% for a bandwidth of 400 Hz can be found in **Table 4**.

From the results presented in **Table 4**, the best possible configuration in terms of bit rate and cumulative density function of BER is the proposal with a bit time of 50 ms, in close competence with the proposal of 30 ms. The PSK using 50 ms was finally chosen because the ratio between the bit rate and the spectral efficiency against the BER was slightly higher than the same metric for 30 ms. That configuration was finally proposed to implement the high throughput mode of the oblique Antarctic transmission system.

4.2 Modulations for NVIS

The transmission system using NVIS has to be power efficient in order to attain the requirements of the battery. The tests performed are designed to optimize the required power for bit rates lower than 3 kbps, which cover the major part of remote sensing applications. The tests compare the performance of simple modulations, that is, 2-FSK, 2-PSK, 4-FSK, and 4-QAM (quadrature amplitude modulation), to find out the best modulation to be used with low transmission power, from 0.3 to 24 W. The duration for each test is adjusted so as the same amount of bits is sent for each modulation. The occupied bandwidth is 2.3 kHz to be consistent with the most common HF standards [30]. The results presented are derived from a 4-month survey between February and May 2018. The tests were performed between our premises in Barcelona (41°24'33.62" N, 2°7'48.82" E) and a field laboratory in Cambrils (41°4'57.22" N, 1°4'4.61" E) placed 96 km away. The frequency was fixed to 4.5 MHz after a detailed analysis of the ionograms from the Ebre Observatory in Roquetes, situated 80 km from Cambrils. We have only performed the transmissions during the day, so the system only uses one frequency. **Figure 9** shows the cumulative density function of the BER for a transmission power of 0.7 and 24 W. For low power transmission (0.7 W), PSK outperforms the rest of the modulations, presenting a BER less than 10^{-3} the 55% of the time and a BER less than 10^{-2} the 80% of the time. For high power (24 W), 2-FSK, 2-PSK, and 4-PSK behave in the same way, while 4-FSK has a much poorer performance. This is because FSK needs a higher bandwidth in order to keep the carrier spacing, and we have made all the tests under the same conditions.

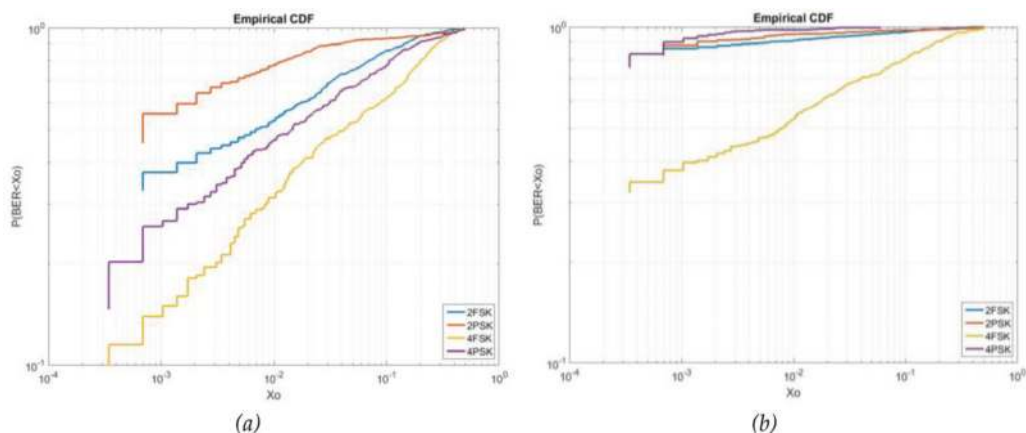


Figure 9. CDF of the BER for an NVIS link with a TX power of 0.7 W (a) and 24 W (b).

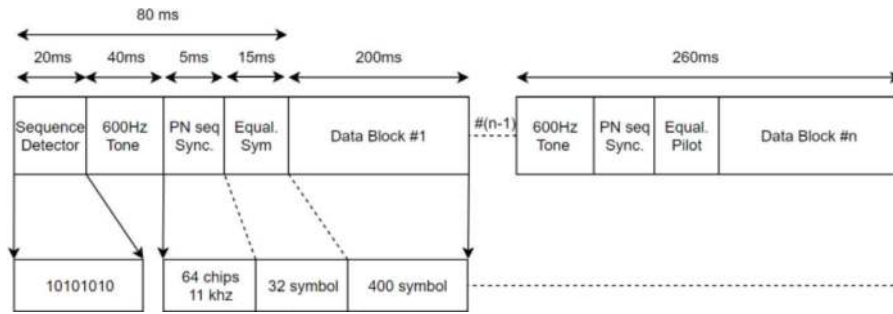


Figure 10.
 Synchronization header for the NVIS frame.

4.3 Signal synchronization

In every telecommunication system, a precise time and frequency synchronization is a key issue in order to receive and demodulate the signal in the best conditions. The classical approach to time synchronization uses a PN sequence, finding the starting point of the frame by simple correlation. In practice, the clock differences between transmitter and receiver as well as the Doppler introduced by the channel may cause frequency shifts up to ± 50 Hz. It follows that the received signal is rotated in phase and, therefore, hampers the correlation. An initial frequency synchronization in narrowband has to be done first. Hence, a tone of 600 Hz (with respect to the carrier) is added to detect which global frequency appears during the signal transmission. A tone of 600 Hz is often masked by the huge levels of noise and interference that are typical in the HF band. Therefore, we need a way to detect in a robust way that the signal is present with a low probability of false alarm. A known sequence of appearance of the 600 Hz tone is added at the beginning of the frame. Once the frequency shift is corrected, next step is synchronization. As the low-cost hardware is limited in speed, memory capacity, and programmable space of the FPGA, the design of the PN sequence is based on achieving correlation with the use of the smallest possible size, in the fastest way and requiring the minimum memory. A PN m-sequence of order 6 (64 chips) and 11 kHz of bandwidth was selected. The final header structure can be seen in **Figure 10**.

5. Protocols for sensor networks in Antarctica

The development of a wide area network of sensors around the Spanish Antarctic Station (or SAS) needs not only a robust physical layer, but also a robust protocol able to provide reliability, security, and tolerance to latency. In fact, we can see a remote sensor in Antarctica as a particular case of the Internet of Things paradigm. In this context, it is not wise to extend the traditional networking infrastructure based on routers to these networks for cost, efficiency, and protocol complexity reasons.

The presented work deals with the issues of utmost importance to achieve quality of service-aware (QoS-aware) communication in wireless and wired sensor networks based on standard communication protocols for the sensor networks around the SAS. The network consists of a system of distributed sensor nodes that interact among them and with infrastructure depending on applications in order to acquire, process, transfer, and provide information extracted from the physical world [31]. Those sensor nodes can be located anywhere and form an ad hoc network, which does not require a communication infrastructure. Sensor nodes are small enough to guarantee pervasiveness in the

Antarctic environment and may be able to observe a certain phenomenon, measure its physical properties, quantify this observation, and finally, transmit gathered data. Sensor nodes could also have processing and routing capabilities using either a wireless or a wired medium. In this environment, sensor networks must dynamically provide the necessary QoS depending on the type of information transmitted by sensor nodes in a multihop topology, and then, the information should be transmitted to central station through NVIS by implementing a delay tolerant network.

As the network is composed of an extensive mesh of spread nodes, they must be located in the same link layer domain to communicate among themselves. Therefore, they will use link layer mechanisms instead of network layer techniques such as IP networks or routing protocols. Consequently, communications become faster and time response turns tighter.

Each type of data may require specific requirements, for example, a critical alarm may demand strict real-time requirements while monitoring reports may not need latency requirements. In order to face these demands, network architecture must deal with several QoS profiles and it should allow discriminating and/or enforcing specific traffic differentiation.

Taking all the above into account, the ICT requirements identified for the system are as follows:

- Distributed system: the system itself is to be distributed and it must allow distributed applications.
- Simplicity: the number of protocols and APIs, and the number of different types of interfaces are kept to a minimum.
- Open system: open to other technologies (future proof) by applying existing standards whenever possible to avoid as much as possible proprietary solutions.
- High interoperability: intertechnology mesh networking between personal area network (PAN) and NVIS backhaul.
- Easy configuration: automatic neighbor discovery and plug and play capability.
- Security: security confinement (to avoid the spreading of vulnerabilities).

Due to the large scenario in which the research project is going to be deployed, different technologies will be needed in order to cover all the areas. Some technologies based on IEEE 802.15.4 are presented as wireless communication candidate technologies that work within mesh networks and they are useful for Antarctic local area network coverage. The result has to be able to support large, geographically diverse networks with minimal infrastructure, with potential millions of fixed endpoints. In the upper layers, there may be technologies such as Zigbee or 6LoWPAN.

When working at Layer2 (second layer of the open system interconnection protocol stack), the communication between two different technology domains (IEEE 802.15.4 and NVIS) involves a gateway, enabling the communication between two separate IEEE 802.15.4 domains across a NVIS domain. A Layer2 routing multihop algorithm capable of working over the obtained topology database is needed in complex network topologies. The multihop algorithm is in charge of determining the neighbors to reach a destination, and the communication with that destination will be requested from the link layer. It is important to bear in mind that the information used by the multihop algorithm can be filtered by the topology control algorithm (valid/nonvalid neighbors).

6. Conclusions and other applications

In this chapter, we have reviewed all the recent activities around the application of HF communications for the research community in Antarctica. The long-range transequatorial link aims to communicate the Antarctic station directly to the home country as an alternative to satellite communications for low bit rate applications. For a transmission power up to 250 W, two different transmission modes have been developed, the robust mode and the high throughput mode. The robust mode, which uses spread spectrum modulation, is suited for extreme channel conditions and achieves 85 bps for a bandwidth of 16 kHz for the spread signal. The high throughput mode, which uses multicarrier modulation and achieves 370 bps for a bandwidth of 400 Hz, is suited for good channel conditions. Although these bit rates are low, they are enough for most of the current sensors installed around the Antarctic stations.

The NVIS link can provide coverage in a surface of approximately 200–250 km radius without the need of line of sight. The main goal of the proposed system is to extend the influence area of the Antarctic stations with the deployment of a wide-area sensor network. When the sensors are distributed in distant zones, it is a hard work to collect the data regularly, and the data are often accessed once or twice a year. With the NVIS solution, all the researchers may get a report of the sensor data in the SAS every day, with no need of direct vision between the sensor and the SAS. The NVIS node has an internal memory that stores the data until the ionosphere conditions allow the transmission. The nodes are intended to be battery powered so the transmission power is kept to a minimum (below 10 W). For NVIS links, the bit rate ranges from 2.3 to 4.6 kbps, depending on channel conditions. On this basis, digital voice and low-resolution images can be sent apart from data from most of the sensors available on the market.

In addition to the use in the Antarctica or any other remote places, NVIS communications have a straightforward application in case of natural disasters, terrorist acts, and communications for developing countries. During a natural disaster or terrorist attack, all the conventional communication systems such as GPRS, 3G, and 4G can be seriously damaged and the communication systems will stop working properly. Our proposed NVIS system may help sanitary assistants, firefighters, police, and other emergency services to communicate during the event of a disaster. In that case, the ease in putting this system up and not needing direct vision between the nodes would be a good solution to save lives.

On the other hand, some parts of the world do not have any communication infrastructures, either because they are uninhabited areas or simply because people cannot afford the price of a conventional communication system. In places where there is no any telecom operator, the communication can only be made via HF and satellite. The NVIS system, based on a low-cost platform, allows the population of developing countries to have access to primary services, such as e-health and education.

Finally, there is a great deal of applications, which can use the proposed communication protocol architecture. They can be classified in detection (e.g., detection of temperatures exceeding a particular threshold, of unauthorized access), tracking (e.g., the tracking of workers in dangerous work environments), and monitoring (e.g., monitoring of inhospitable environments).

Author details

Joaquim Porté, Joan Lluís Pijoan*, Josep Masó, David Badia, Agustín Zaballos and Rosa Maria Alsina-Pagès
La Salle in Ramon Llull University, Barcelona, Spain

*Address all correspondence to: joanlluis.pijoan@salle.url.edu

IntechOpen

© 2018 The Author(s). Licensee IntechOpen. This chapter is distributed under the terms of the Creative Commons Attribution License (<http://creativecommons.org/licenses/by/3.0>), which permits unrestricted use, distribution, and reproduction in any medium, provided the original work is properly cited. 

References

- [1] Davies K. Ionospheric Radio. Michael Faraday House, Six Hills Way, Stevenage SG1 2AY, UK: The Institution of Engineering and Technology, IET; 1990. Available from: <http://digital-library.theiet.org/content/books/ew/pbew031e>
- [2] Witvliet BA, Alsina-Pagès RM. Radio communication via near vertical incidence skywave propagation: An overview. *Telecommunication Systems*. 2017;**66**(2):295-309. Available from: <http://link.springer.com/10.1007/s11235-017-0287-2>
- [3] Watterson C, Juroshek J, Bensema W. Experimental confirmation of an HF channel model. *IEEE Transactions on Communications*. 1970;**18**(6):792-803. Available from: <http://ieeexplore.ieee.org/document/1090438/>
- [4] Mastrangelo JF, Lemmon JJ, Vogler LE, Hoffmeyer JA, Pratt LE, Behm CJ. A new wideband high frequency channel simulation system. *IEEE Transactions on Communications*. 1997;**45**(1):26-34. Available from: <http://ieeexplore.ieee.org/document/554283/>
- [5] Cannon PS, Angling MJ, Davies NC, Wilink T, Jodalen V, Jacobson B, et al. Damson HF channel characterisation-a review. In: *MILCOM 2000 Proceedings 21st Century Military Communications Architectures and Technologies for Information Superiority* (Cat No00CH37155). IEEE. pp. 59-64. Available from: <http://ieeexplore.ieee.org/document/904913/>
- [6] Davies NC, Willink TJ, Angling MJ, Cannon PS. Initial Results from WHISPER; a Wideband HF Ionospheric Sounder for Propagation Environment Research. 2001. Available from: <https://researchportal.bath.ac.uk/en/publications/initial-results-from-whisper-a-wideband-hf-ionospheric-sounder-fo>
- [7] Angling MJ, Cannon PS, Davies NC, Willink TJ, Jodalen V, Lundborg B. Measurements of Doppler and multipath spread on oblique high-latitude HF paths and their use in characterizing data modem performance. *Radio Science*. 1998;**33**(1):97-107. DOI: 10.1029/97RS02206
- [8] Hervás M, Alsina-Pagès R, Orga F, Altadill D, Pijoan J, Badia D. Narrowband and wideband channel sounding of an antarctica to spain ionospheric radio link. *Remote Sensing*. 2015;**7**(9):11712-11730. Available from: <http://www.mdpi.com/2072-4292/7/9/11712>
- [9] Ads AG, Bergadà P, Regué JR, Alsina-Pagès RM, Pijoan JL, Altadill D, et al. Vertical and oblique ionospheric soundings over the long haul HF link between Antarctica and Spain. *Radio Science*. 2015;**50**(9):916-930. DOI: 10.1002/2015RS005773
- [10] Pijoan J, Altadill D, Torta J, Alsina-Pagès R, Marsal S, Badia D. Remote geophysical observatory in antarctica with HF data transmission: A review. *Remote Sensing*. 2014;**6**(8):7233-7259. Available from: <http://www.mdpi.com/2072-4292/6/8/7233>
- [11] Ads AG, Bergadà P, Vilella C, Regué JR, Pijoan JL, Bardají R, et al. A comprehensive sounding of the ionospheric HF radio link from Antarctica to Spain. *Radio Science*. 2013;**48**(1):1-12. DOI: 10.1029/2012RS005074
- [12] Vilella C, Miralles D, Pijoan JL. An Antarctica-to-Spain HF ionospheric radio link: Sounding results. *Radio Science*. 2008;**43**(4):n/a. DOI: 10.1029/2007RS003812
- [13] Alsina-Pagès R, Hervás M, Orga F, Pijoan J, Badia D, Altadill D. Physical layer definition for a long-haul

HF Antarctica to Spain radio link. Remote Sensing. 2016;**8**(5):380. Available from: <http://www.mdpi.com/2072-4292/8/5/380>

[14] Hervás M, Alsina-Pagès RM, Pijoan JL, Salvador M, Badia D. Advanced modulation schemes for an Antarctic Long Haul HF Link. Telecommunication Systems. 2016;**62**(4):757-770. Available from: <http://link.springer.com/10.1007/s11235-015-0110-x>

[15] Alsina-Pagès RM, Salvador M, Hervás M, Bergadà P, Pijoan JL, Badia D. Spread spectrum high performance techniques for a long haul high frequency link. IET Communications. 2015;**9**(8):1048-1053 Available from: <http://digital-library.theiet.org/content/journals/10.1049/iet-com.2014.0807>

[16] Hervás M, Pijoan JL, Alsina-Pagès RM, Salvador M, Badia D. Single-carrier frequency domain equalisation proposal for very long haul HF radio links. Electronics Letters. 2014;**50**(17):1252-1254. Available from: <http://digital-library.theiet.org/content/journals/10.1049/el.2014.1184>

[17] Bergadà P, Alsina-Pagès RM, Pijoan JL, Salvador M, Regué JR, Badia D, et al. Digital transmission techniques for a long haul HF link: DSSS versus OFDM. Radio Science. 2014;**49**(7):518-530. DOI: 10.1002/2013RS005203

[18] Orga F, Hervas M, Alsina-Pages RM. Flexible low-cost SDR platform for HF communications: Near vertical incidence skywave preliminary results. IEEE Antennas and Propagation Magazine. 2016;**58**(6):49-56. Available from: <http://ieeexplore.ieee.org/document/7605405/>

[19] Libelium—Connecting Sensors to the Cloud [Internet]. [cited 2018 Jul 6]. Available from: <http://www.libelium.com/>

[20] Ionogrames de Livingston [Internet]. 2018. Available from: <http://www.obsebre.url.edu/ca/ionogrames-de-livingston>

[21] LDI, Lowell Digisonde International (Digisonde.com) [Internet]. 2018. Available from: <http://www.digisonde.com/stationlist.html>

[22] Witvliet BA. Near Vertical Incidence Skywave. Enschede, The Netherlands: University of Twente; 2015

[23] Witvliet BA, van Maanen E, Petersen GJ, Westenberg AJ, Bentum MJ, Slump CH, et al. Near vertical incidence skywave propagation: Elevation angles and optimum antenna height for horizontal dipole antennas. IEEE Antennas and Propagation Magazine. 2015;**57**(1):129-146. Available from: <http://ieeexplore.ieee.org/document/7047674/>

[24] Solar Cycle progression|Solar activity|SpaceWeatherLive.com [Internet]. 2018. Available from: <https://www.spaceweatherlive.com/en/solar-activity/solar-cycle>

[25] LDI, Lowell Digisonde International Station List (Digisonde.com) [Internet]. 2018. Available from: <http://www.digisonde.com/stationlist.html>

[26] Proakis JG. Digital communications. 4th ed. New York: McGraw-Hill; 2001

[27] Lavers C. Essential Sensing and Telecommunications for Marine Engineering Applications. 1st ed. London: Bloomsbury Publishing; 2017

[28] Hervas M, Pijoan JL, Alsina-Pagès R, Salvador M, Altadill D. Channel sounding and polarization diversity for the NVIS channel. Faro, Sweden: Nordic HF 13; Aug 2013

[29] Gold R. Optimal binary sequences for spread spectrum multiplexing (Corresp.). IEEE Transactions on

Information Theory. 1967;**13**(4):619-621.
Available from: <http://ieeexplore.ieee.org/document/1054048/>

[30] MIL-188-110A [Internet]. 2018.
Available from: <http://www.wavecom.ch/content/ext/DecoderOnlineHelp/default.htm#!worddocuments/mil188110a.htm>

[31] Caballero V, Vernet D, Zaballos A, Corral G. Prototyping a web-of-energy architecture for smart integration of sensor networks in smart grids domain. *Sensors*. 2018;**18**(2):400.
Available from: <http://www.mdpi.com/1424-8220/18/2/400>